NASA TN D-293

TECHNICAL NOTE

D-293

PERFORMANCE OF SEVERAL METHOD-OF-CHARACTERISTICS EXHAUST NOZZLES

By John M. Farley and Carl E. Campbell

Lewis Research Center
Cleveland, Ohio

NATIONAL AERONAUTICS AND SPACE ADMINISTRATION
WASHINGTON
October 1960

NATIONAL AERONAUTICS AND SPACE ADMINISTRATION

TECHNICAL NOTE D-293

PERFORMANCE OF SEVERAL METHOD-OF-CHARACTERISTICS EXHAUST NOZZLES

By John M. Farley and Carl E. Campbell

SUMMARY

Nozzle performance data were obtained with three "method-of-characteristics" nozzles and a 15° conical nozzle at pressure ratios up to 130. Each basic configuration was cut off and tested at expansion ratios of 25, 20, 15, and 10. Unheated dry air was used at nozzle inlet pressures up to 22,000 pounds per square foot absolute. Nozzle thrust data were extrapolated to infinite pressure ratio (zero discharge pressure).

As much as 1-percent increase in thrust, with no increase in nozzle surface area (weight), can be obtained by using a method-of-characteristics nozzle instead of a 15° conical nozzle when operating with a nozzle expansion ratio of 25 and nozzle pressure ratios from 200 to ∞. Conversely, for the same thrust, reductions in nozzle divergent surface area in the order of 25 percent are possible. The thrust performance of the method-of-characteristics nozzle was not as good as that of the 15° conical nozzle when operating at pressure ratios considerably below design (below 100 for the expansion ratio 25 nozzles). Theoretical and measured nozzle momentum coefficients agreed within about 0.6 percent. This is the order of accuracy of both the measured and theoretical values.

INTRODUCTION

Because of the high ratio of missile gross weight to payload weight required for space missions, the efficiency and weight of the propulsion system can have a large effect on payload. If, for example, the payload weight is 1 percent of the gross weight, a 1-percent increase in exhaust-nozzle efficiency would allow the payload to be almost doubled. Conversely, if the nozzle were reduced in length with no reduction of efficiency, the savings in nozzle weight could be applied directly to the payload.

Analytic studies have indicated (refs. 1 and 2) that, with nozzle expansion ratios of about 25, increases in design-point efficiency on the order of 1 percent may be obtained by using an isentropic contoured nozzle in place of a 15° conical nozzle of the same length; or for the same design-point efficiency, the contoured nozzle can be about 20 percent shorter than the conical nozzle. In order to demonstrate experimentally the thrust-weight gains possible with isentropic contoured nozzles (as compared with a 15° nozzle), the experimental investigation reported herein was undertaken. It was also desired to determine the performance of this type nozzle when operating below design pressure ratio. Air, rather than rocket gases, was used as the test fluid in order to allow more precise measurements and to eliminate uncertainties due to gas-state changes.

Coordinates for the three basic nozzles investigated were calculated by the method of characteristics and were obtained from reference 3. These nozzle contours were designed to give uniform parallel exit flow at Mach numbers of 5.018, 5.819, and 6.851; however, only the portions up to an expansion ratio of 25 were constructed. (In spite of this, the basic nozzle configurations shall hereinafter be referred to by the nominal design Mach numbers of 5.02, 5.82, and 6.85.) For comparison, a 15° conical nozzle was also investigated. All the basic nozzles were constructed in sections so that they could be run at nominal expansion ratios ranging from 10 to 25.

The investigation was conducted in an NASA Lewis Research Center altitude facility with unheated dry air (less than 1 grain of water per pound of air) over a range of pressure ratios from about 10 to 130. Data were obtained with nominal inlet total pressures of 12,000 and 22,000 pounds per square foot.

APPARATUS

Nozzle Configurations

Figure 1 is a photograph of a typical nozzle installed in the test facility. The wooden nozzles were built in sections giving nominal area ratios of 10, 15, 20, and 25. After rough machining, the sections were bolted together for finishing.

Initial nozzle coordinates (not corrected for boundary-layer displacement) were obtained from reference 2. The nozzles of reference 2 were designed with zero wall radius of curvature at the throats. In order to comply more closely with current rocket nozzle practice, the 8/10 streamlines of these nozzles were used, resulting in a wall radius of curvature of approximately 8/10 of the nozzle throat diameter. The final nozzle coordinates (fig. 2) include corrections for boundary-layer displacement thickness (fig. 3), which were computed by the methods

given in reference 4. Figure 4 is a sketch of the 15° conical nozzle. The subsonic portions of the method-of-characteristics nozzles were the same as those of the 15° nozzle. All nozzles had a nominal throat diameter of $4\frac{3}{4}$ inches. As an indication of relative nozzle weights, the variation of nozzle surface area ratio S/A_{cr} with nozzle expansion ratio A/A_{cr} is presented in figure 5.

Installation and Instrumentation

Figure 6 is a sketch of the nozzle test installation showing thrust-measurement linkage and location of instrumentation. Location of the nozzle static-pressure instrumentation is shown in figure 4. In terms of nozzle area ratio, the location of nozzle static-pressure instrumentation was the same for all nozzles.

PROCEDURE

Each nozzle was first tested with maximum expansion ratio (25). The last section of the nozzle was then removed and data were obtained with an expansion ratio of 20. This procedure was followed until data had been obtained at expansion ratios of 25, 20, 15, and 10. Each configuration was investigated over a range of pressure ratios from about 10 to 130 with a nominal inlet pressure of 22,000 pounds per square foot. With most of the configurations, data were also obtained with an inlet pressure of 12,000 pounds per square foot to determine possible effects of Reynolds number. Symbols used in the report are listed in appendix A.

RESULTS AND DISCUSSION

Nozzle Flow Coefficients

Essentially all of the flow-coefficient values obtained were well within ±0.5 percent of 0.995 (fig. 7). No effect of pressure level is apparent within the data scatter.

Comparison of Measured and Theoretical Nozzle Performance

Nozzle total momentum. - When a nozzle is flowing full, the total momentum at the nozzle exit is independent of the ambient pressure, and the net thrust coefficient can be written in the form

$$C_F \equiv \frac{F_n}{\varphi A_{cr} P_N} = C_M - \frac{p_a}{P_N} \frac{A_e}{A_{cr}} \frac{1}{\varphi} \qquad (1)$$

where C_M is the exit total momentum coefficient (or thrust coefficient of the nozzle discharging into a vacuum) and $(p_a/P_N)(A_e/A_{cr})(1/\varphi)$ corrects for the pressure into which the nozzle is discharging.

Because it is independent of pressure ratio (as long as the nozzle is flowing full), C_M is an excellent parameter for comparison of nozzles. Values of C_M were calculated for each nozzle expansion ratio using equation (1) and measured values of C_F obtained only when the nozzles were flowing full. A typical plot of C_M against nozzle pressure ratio is presented in figure 8. For each configuration, the values of C_M were constant within a scatter of about ±0.5 percent.

A cross plot showing the variation of C_M with nozzle expansion ratio for all the nozzle designs is presented in figure 9. The data points on this figure represent the average measured values obtained from plots such as figure 8. Also included in figure 9 are theoretical curves of C_M for the method-of-characteristics nozzles, which were computed from the theoretical nozzle pressure distributions. These theoretical curves also include corrections for boundary-layer effects. (The calculation methods are discussed in appendix B.) For the 5.82 and 6.85 Mach number nozzles, the experimental values and the theoretical curves agree well within the scatter of the experimental data. The theoretical curve for the 5.02 Mach number nozzle is about 0.01 (0.6 percent) higher than the average experimental values. Reasons for the larger discrepancy in the latter case have not been resolved. Consideration of calibration and measurement accuracies indicated that the faired experimental values are accurate to within ±0.5 percent. Possible contributing causes are (1) underestimation of boundary-layer losses and (2) interpolation errors in the theoretical pressure distribution. (Flow conditions were calculated at only a few axial stations in ref. 2, so that extensive interpolation was required.)

The increase in thrust with decreasing nozzle design Mach number that is indicated in figure 9 occurs because, for a given expansion ratio, the lower the nozzle design Mach number, the closer the exit flow is to being uniform and axial. (The 5.02 nozzle is truncated to a lesser extent than the 5.82 or the 6.85 nozzle.) The additional thrust is therefore obtained with the penalty of additional length and weight.

Values of C_M were also computed from the measured nozzle pressure distributions (see appendix B). The values obtained were from 0.1 to 0.4 percent higher than the values computed from theoretical pressure distributions. In view of the difficulty of obtaining accurate integrations of steep nozzle pressure gradients, this agreement is considered excellent.

Nozzle pressure distributions. - A comparison of theoretical and measured nozzle static-pressure distributions is presented in figure 10.

Each of the data points on figure 10 represents an average of many measurements that generally scattered no more than ±3 percent. With all three of the contoured nozzles, all the average measured pressure ratios were essentially within 0.001 of the theoretical curves. For expansion ratios greater than about 15 (fig. 10(c)), the measured pressure ratios were generally slightly higher than the theoretical curves. This probably indicates that the corrections made for boundary-layer displacement were too small. At an expansion ratio of 24.5, the measured values of wall pressure were approximately 10 percent higher than the theoretical values; however, the absolute pressure level is so low that the effect on thrust coefficient is extremely small.

The generally good agreement between theoretical and experimental values of total momentum coefficients and of nozzle pressure distribution indicates that, if gas properties are adequately known and if boundary-layer effects are considered, the performance of a method-of-characteristics nozzle can be computed to about the same order of accuracy as it can be measured.

Variation of Thrust with Pressure Ratio

Figure 11 shows the variation of nozzle thrust ratio with nozzle pressure ratio for each configuration. Values of $C_F/C_{F,id}$ were extended to pressure ratios up to 1000 by use of equation (1) and the C_M values of figure 9. The vertical line crossing each experimental curve indicates the pressure ratio below which the nozzle flow separates. To avoid confusion, theoretical curves are not shown on figure 11. However, as long as the nozzle is flowing full, the percentage agreement would be about the same as that shown for the momentum coefficient in figure 9.

Comparison of the curves in figure 11 shows that the thrust of the contoured nozzles was not as high as that of the 15° nozzle of the same expansion ratio when operating at pressure ratios considerably below design (below 100 for the expansion ratio 25 configuration). This, of course, means that the overexpansion losses are greater in the contoured nozzles. This difference in overexpansion losses is attributed primarily to differences in the nozzle pressure-area relations that exist in the unseparated-flow portion of the nozzles. Examination of figure 10 shows that, in the downstream portions of the nozzles ($A/A_{cr} > 4.5$), the wall static-pressure ratio p_w/P_N is lower in the conical than in the contoured nozzles at any given expansion ratio. Also, it has been shown (e.g., refs. 5 and 6) that the wall static-pressure ratio at which the flow separates p_s/P_N is dependent primarily upon the nozzle pressure ratio P_N/p_a and is relatively insensitive to configuration. Therefore, with a given nozzle pressure ratio, the flow will separate at a lower expansion ratio in the conical nozzle than in the method-of-characteristics nozzles, resulting in lower overexpansion losses in the conical nozzle.

This is illustrated in the following simplified sketch:

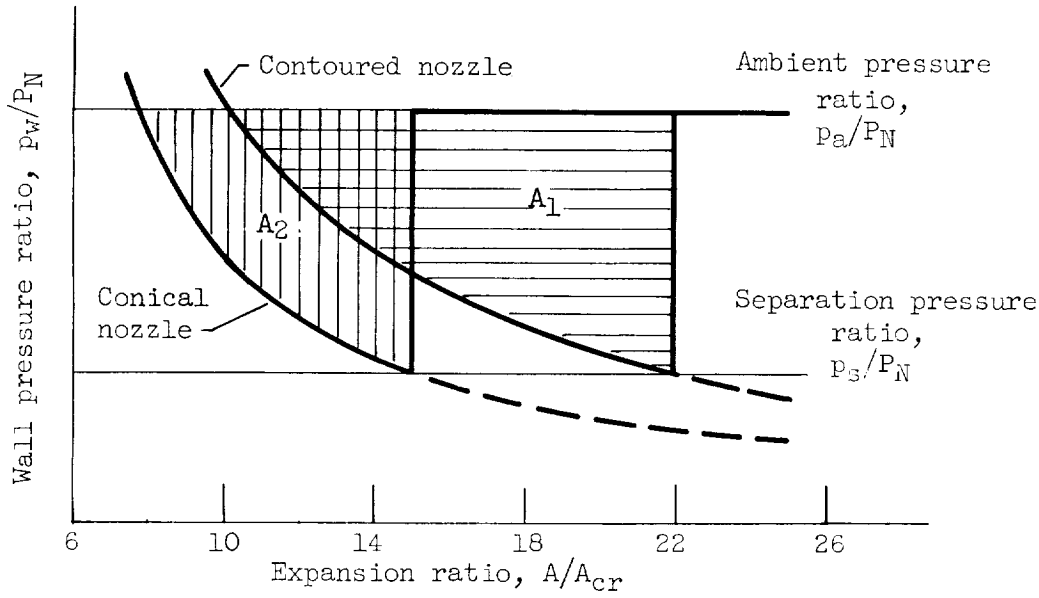

The shaded areas above each curve represent the thrust losses due to overexpansion. For a given ambient pressure ratio, separation occurs at a lower expansion ratio in the conical nozzle, with the result that A_2 is less than A_1.

It will be shown later that, with the method-of-characteristics nozzles, there are secondary effects of configuration on the relation between p_s/P_N and P_N/p_a that are in the direction of causing still more overexpansion (and thus, thrust loss) in the contoured nozzles. Although these thrust losses are undesirable, this greater tendency of the contoured nozzles to overexpand may be an advantage in cases where separation is undesirable for structural or control reasons, and the engine must operate at reduced pressure ratio for only a relatively short time.

It can also be seen in figure 11 that the peaks in the $C_F/C_{F,id}$ curves do not necessarily occur at the design-point pressure ratios (solid symbols). This is a result of the definitions of design pressure ratio and of $C_F/C_{F,id}$. In this paper, the design point is taken as the condition for which the measured wall static pressure at the nozzle exit is equal to the ambient pressure ($p_e/P_N = p_a/P_N$). Thrust ratio is given by

$$\frac{C_F}{C_{F,id}} = \frac{C_M - \frac{p_a}{P_N}\frac{A_e}{A_{cr}}\frac{1}{\varphi}}{\frac{mV_{id}}{P_N A_{cr}}} \qquad (2)$$

where, with fixed configuration and inlet conditions, C_M, φ, A_e/A_{cr}, and $m/P_N A_{cr}$ are all constant.

The pressure ratio at which the maximum value of $C_F/C_{F,id}$ will be obtained may be found by differentiating the equation for $C_F/C_{F,id}$ with respect to pressure ratio and setting the result equal to zero. This operation results in the following relation:

$$C_M - \frac{p_a}{P_N}\frac{A_e}{A_{cr}}\frac{1}{\varphi}\left(1 + \gamma M_{id}^2\right) = 0 \qquad \text{when} \quad C_F/C_{F,id} = \text{maximum} \tag{3}$$

Ideal total momentum coefficient is given by

$$C_{M,id} = \frac{(pA + mV)_{id}}{P_N \varphi A_{cr}} = \frac{p_a}{P_N}\left(\frac{A}{A_{cr}}\right)_{id}\frac{1}{\varphi}\left(1 + \gamma M_{id}^2\right) \tag{4}$$

Combining these equations results in

$$\frac{C_M}{C_{M,id}} = \frac{A_e/A_{cr}}{(A/A_{cr})_{id}} \qquad \text{when} \quad C_F/C_{F,id} = \text{maximum} \tag{5}$$

For an imperfect nozzle, $C_M < C_{M,id}$, and therefore $A_e/A_{cr} < (A/A_{cr})_{id}$. Furthermore, the values of p_e/P_N, for all configurations tested, were higher than the one-dimensional values for the nozzle expansion ratios. It can therefore be concluded that the nozzle pressure ratio P_N/p_a at which the $C_F/C_{F,id}$ curves peak will be higher than the "design" pressure ratio P_N/p_e.

A cross plot of design values of $C_F/C_{F,id}$ against design pressure ratio is presented in figure 12. For the 15° conical nozzle, $C_F/C_{F,id}$ is essentially constant at 0.98; whereas, for the contoured nozzles, $C_F/C_{F,id}$ varies from 0.99 ($M = 5.02$, $A_e/A_{cr} = 25$ nozzle) to 0.95 ($M = 6.85$, $A_e/A_{cr} = 10$ nozzle). The variations obtained with the contoured nozzle occur because the exit flow is less uniform and less axial as the nozzle lengths are reduced from the full design length. On the other hand, essentially radial flow is established a short distance downstream of the throat in the conical nozzle, so that reducing nozzle length has little effect on the flow distribution or angularity.

Nozzle Flow Separation

Pressure distributions. - Typical nozzle pressure-distribution curves (with flow separation) are presented in figure 13; figure 13(a) shows data obtained with the 5.82 nozzle and figure 13(b) shows data for the 5.02 nozzle. Data obtained with the 15° conical nozzle and the 6.85 contoured nozzle gave essentially the same shaped curves and slopes as illustrated in figure 13(a). With the 5.02 nozzle (fig. 13(b)), some difference was observed: With an expansion ratio of 25, and to a lesser extent with 20, additional pressure rise occurred downstream of the pressure rise at separation (e.g., the curves obtained with nozzle pressure ratios of 0.0288, 0.0425, 0.0535, and 0.0864, in fig. 13(b)). This possibly indicates flow reattachment in the downstream portion of the nozzle resulting from the low divergence angles (3° to 6°) in this region.

Separation pressure-rise ratio. - Figure 14 shows the variation of the static-pressure-rise ratio at separation p_a/p_s with the separation wall static-pressure ratio p_s/p_N. Values of p_s/P_N were obtained from plots such as figure 13, and are the values of wall static pressure at which separation commences. Included on figure 14 are theoretical lines of pressure-rise ratio for oblique shock waves having constant Mach number ratio across the shock wave. Except for variations (dashed lines on fig. 14) near the exit of each nozzle, the data for each nozzle design generalize independently of nozzle expansion ratio. The deviations that occur near the exit of each nozzle are caused by feedback of the ambient pressure through the subsonic portion of the nozzle boundary layer. Such feedback causes the nozzle exit wall static pressure to approach (and vary with) ambient pressure, even when the nozzle flow is not separated. For the 15° conical nozzle (fig. 14(a)), the generalized curve of separation pressure-rise ratio coincides with the curve for a Mach number ratio of 0.76 across an oblique shock wave. This agrees with the data of reference 5, which were obtained with 15°, 25°, and 30° conical nozzles, and also with the value suggested in reference 6.

For the contoured nozzles (fig. 14(b)), the separation pressure-rise ratio did not generalize with Mach number ratio. Since separation pressure ratio is primarily a function of boundary-layer characteristics, these data may indicate that the boundary layers in the conical and in the contoured nozzles are significantly different. The Mach 5.02 nozzle separation pressure-ratio plot (fig. 14(b)) shows more scatter than the others. This may be a result of the flow reattachment that occurred in this nozzle.

Thrust-Weight Comparison of Nozzle Configurations

Figure 15 shows the variation of $C_F/C_{F,id}$ with surface area ratio (weight) for nozzle pressure ratios P_N/p_a of infinity, 500, and 200. In the pressure-ratio range from 200 to ∞, and with surface area ratios greater than 50, one or more of the method-of-characteristics nozzles gave performance equal to or better than the 15° conical nozzle. For example, with a surface area ratio of 95, the Mach 5.82 nozzle would give about 1 percent more thrust than the conical nozzle over the pressure-ratio range from 200 to ∞. In this case, the expansion ratio for both nozzles is about 25. If, on the other hand, a set thrust level is desired, considerable weight saving can be obtained by using a contoured nozzle. For example, at a pressure ratio of infinity the Mach 5.82 nozzle having a surface area ratio of 70 would give the same thrust as a 15° conical nozzle having a surface area ratio of 90. At a pressure ratio of 200, the same Mach 5.82 nozzle would have more than 1 percent greater thrust than the same 15° conical nozzle. The dropoff in nozzle performance at the higher surface area ratios indicated in figure 15(c) occurs because, with a nozzle pressure ratio of 200, the larger-area-ratio nozzles are operating overexpanded and therefore less efficiently.

Figure 16 is similar to figure 15, except that nozzle length rather than nozzle surface area is used as the basis of comparison. This comparison also shows that savings in length can generally be obtained by use of a contoured nozzle.

SUMMARY OF RESULTS

The results of an investigation of three method-of-characteristics nozzles and a 15° conical nozzle are as follows:

1. For expansion ratio of 25 and nozzle pressure ratios from 200 to ∞, as much as 1-percent increase in thrust, with no increase in nozzle surface area (weight), can be obtained by using a method-of-characteristics nozzle instead of a 15° conical nozzle. Conversely, for the same thrust, reductions in nozzle divergent surface area in the order of 25 percent are possible.

2. At low operating pressure ratios, flow in the method-of-characteristics nozzles overexpanded to a greater extent than that in the 15° conical nozzle. Although this results in reduced thrust, it may be an advantage in cases where flow separation is undesirable for structural or control reasons.

3. Theoretical and measured nozzle momentum coefficients agreed within about 0.6 percent. This is the order of accuracy of both the measured and theoretical values.

Lewis Research Center
National Aeronautics and Space Administration
Cleveland, Ohio, April 1, 1960

E-581

APPENDIX A

SYMBOLS

Any consistent set of dimensions may be used.

A	cross-sectional area
C_F	nozzle thrust coefficient, $F_n/\varphi A_{cr} P_N$
$C_F/C_{F,id}$	nozzle thrust ratio, $F/mV_{id} = C_F/\left[(p/P)(A/A_{cr})\gamma M^2\right]_{p_a/P_N}$
C_M	nozzle total momentum coefficient, $C_F + (p_a/P_N)(A_e/A_{cr})(1/\varphi)$
F	thrust
M	Mach number
m	mass flow
P_N	nozzle inlet total pressure
p	static pressure
p_a	ambient (nozzle discharge) pressure
p_e	nozzle exit wall static pressure
p_s	nozzle wall static pressure at separation
p_w	local nozzle wall static pressure
r	radius
S	nozzle divergent surface area
V	velocity
w	weight flow
x	axial distance from nozzle throat
γ	ratio of specific heats, 1.4
δ^*	boundary-layer displacement thickness

θ boundary-layer momentum thickness

φ nozzle throat flow coefficient, $w_1/w_{cr,id}$

Subscripts:

bl boundary layer

cr throat or critical (M = 1) conditions

e nozzle exit station

id ideal (one-dimensional) value

n net

s separation

x arbitrary nozzle station

1 airflow measuring station

APPENDIX B

THEORETICAL NOZZLE THRUST CALCULATIONS

Nonviscous Thrust

If skin friction is neglected, total momentum coefficient at any station x in the nozzle can be found from

$$C_M = C_{M,cr} + \left[\int_1^{A_x'/A_{cr}} \frac{p_w}{P_N}\, d\left(\frac{A'}{A_{cr}}\right)\right]\frac{1}{\varphi} \qquad \text{(B1a)}$$

where $C_{M,cr}$ is the total momentum coefficient at the nozzle throat, the integral term is the pressure-area force on the divergent portion of the nozzle, and A' is the nozzle cross-sectional area not corrected for boundary-layer displacement. With a method-of-characteristics nozzle, the relation between p_w/P_N and A'/A_{cr} is known, and therefore the integral term can be evaluated graphically.

Theoretical Thrust Corrected for Boundary-Layer Losses

The flow areas of the method-of-characteristics nozzles tested were corrected for boundary-layer displacement, so that the variation of p_w/P_N with nozzle length is the same as for the calculated nonviscous case. The flow-area correction is given by

$$\Delta A_x = 2\pi r_x \delta_x^*$$

Theoretical variations of p_w/P_N with A/A_{cr} (A/A_{cr} corrected for boundary-layer displacement) are shown in figure 10 for the method-of-characteristics nozzles.

To obtain total momentum coefficient with viscous effects, the pressure-area force due to the boundary-layer displacement area is added; and the loss in momentum, due to decreased velocity of the mass flow in the boundary layer, is subtracted from the nonviscous total momentum coefficient. By definition of boundary-layer momentum thickness θ, the loss in momentum due to mass flow in the boundary layer is given by

$$\frac{\Delta(mV)_{bl}}{P_N A_{cr}} = \frac{2\pi r\theta}{A_{cr}} \frac{p_w}{P_N} \gamma M^2$$

where M is the Mach number corresponding to the local wall pressure ratio p_w/P_N. Total momentum coefficient is then given by

$$C_M = C_{M,cr} + \left\{ \int_1^{A_x'/A_{cr}} \frac{p_w}{P_N} d\left(\frac{A'}{A_{cr}}\right) + \frac{[2\pi r\delta^*(p_w/P_N)]_x}{A_{cr}} - \frac{[2\pi r\theta(p_w/P_N)\gamma M^2]_x}{A_{cr}} \right\} \frac{1}{\varphi} \tag{B1b}$$

Boundary-layer displacement thicknesses δ^* were calculated by the methods of reference 4 (assuming a 1/7 power profile), and are plotted in dimensionless form in figure 3. Values of δ^*/θ were obtained from the tables of reference 4, using Mach numbers corresponding to the theoretical values of p_w/P_N and assuming a 1/7 power profile.

E-351

Thrust from Measured Pressure Distribution

The equation for total momentum coefficient can be written

$$C_M = C_{M,cr} + \left[\int_1^{A_x/A_{cr}} \frac{p_w}{P_N} d\left(\frac{A}{A_{cr}}\right) - \frac{\text{Skin friction force}}{P_N A_{cr}} \right] \frac{1}{\varphi} \tag{B2}$$

where the pressure-area integration is carried out using area ratios corrected for boundary-layer displacement.

If it is assumed that skin friction and the throat momentum are the same as in the theoretical calculation, the momentum coefficient can be obtained from the measured pressure distribution by

$$C_M = C_{M,theor} + \frac{1}{\varphi} \int_1^{A_x/A_{cr}} \left(\frac{p_w}{P_{N,meas}} - \frac{p_w}{P_{N,theor}} \right) d\left(\frac{A}{A_{cr}}\right) \tag{B3}$$

Nozzle-Throat Flow and Thrust Coefficients

For all theoretical nozzle thrust calculations, the nozzle flow coefficient φ was assumed to be 0.995; this value is typical for well-designed nozzle inlets and agrees with the measured values obtained with the current nozzles.

By integration of various assumed throat velocity profiles, it can be shown that the ratio of actual to ideal throat total momentum is always larger than the throat flow coefficient. It was, therefore, assumed that the throat total momentum was 0.996 times the one-dimensional momentum for M = 1. Thus,

$$C_{M,cr} = \frac{0.996\left[\frac{p}{P_N}(1+\gamma)\right]_{M=1}}{\varphi} = \frac{(0.996)(1.2679)}{0.995} = 1.269 \qquad (B4)$$

REFERENCES

1. Rao, G. V. R.: Exhaust Nozzle Contour for Optimum Thrust. Jet Prop., vol. 28, no. 6, June 1958, pp. 377-382.

2. Clippinger, R. F.: Supersonic Axially Symmetric Nozzles. Rep. 794, Ballistic Res. Labs., Aberdeen Proving Ground (Md.), Dec. 1951.

3. Rao, G. V. R.: Contoured Rocket Nozzles. Paper presented at Ninth Annual Cong. Int. Astronautical Federation (Amsterdam), Aug. 25-30, 1958.

4. Tucker, Maurice: Approximate Calculation of Turbulent Boundary-Layer Development in Compressible Flow. NACA TN 2337, 1951.

5. Campbell, C. E., and Farley, J. M.: Performance of Several Conical Convergent-Divergent Rocket-Type Exhaust Nozzles. NASA TN D-467, 1960.

6. Reshotko, Eli, and Tucker, Maurice: Effect of a Discontinuity on Turbulent Boundary-Layer-Thickness Parameter with Application to Shock-Induced Separation. NACA TN 3454, 1955.

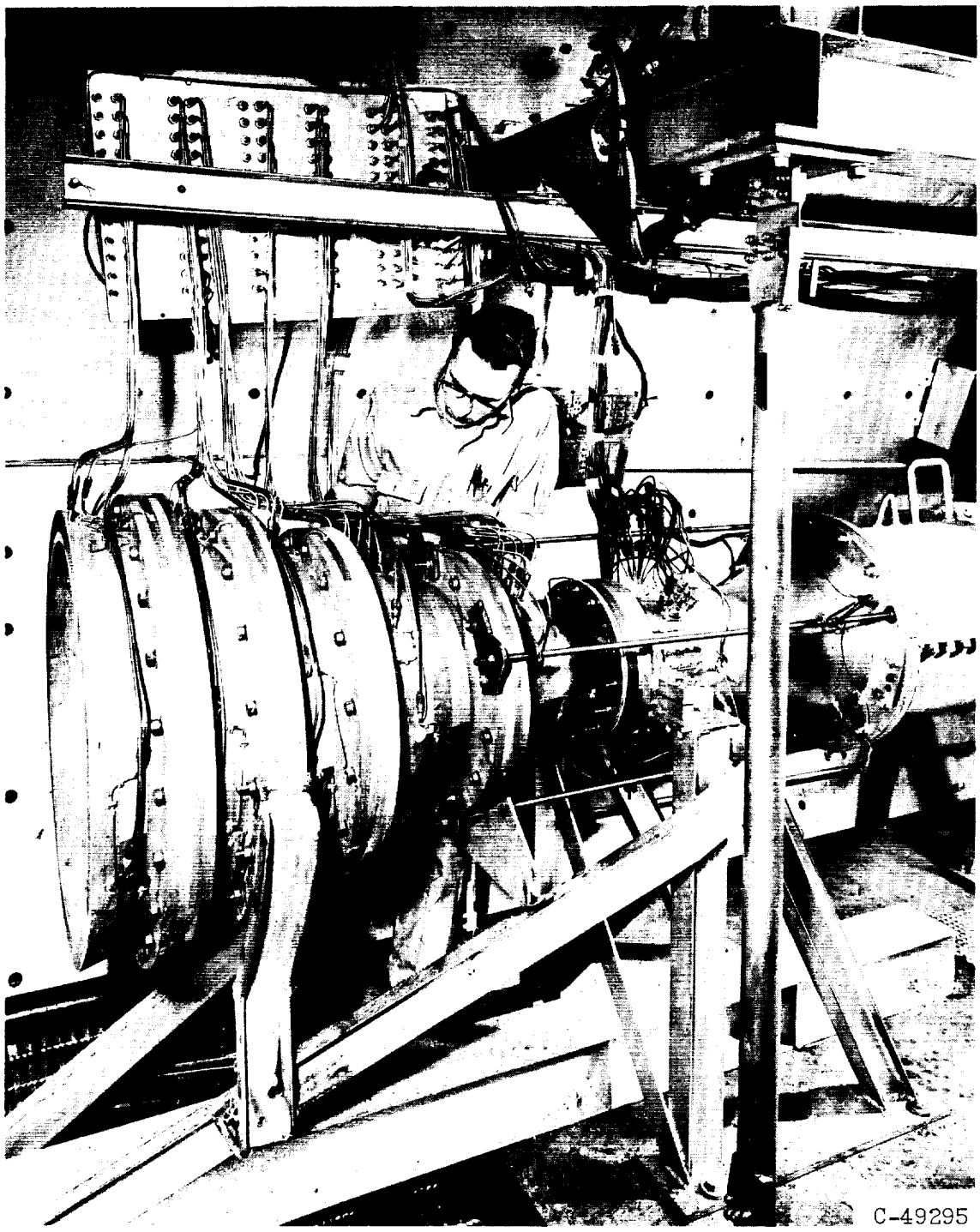

Figure 1. - Typical nozzle installed in test facility.

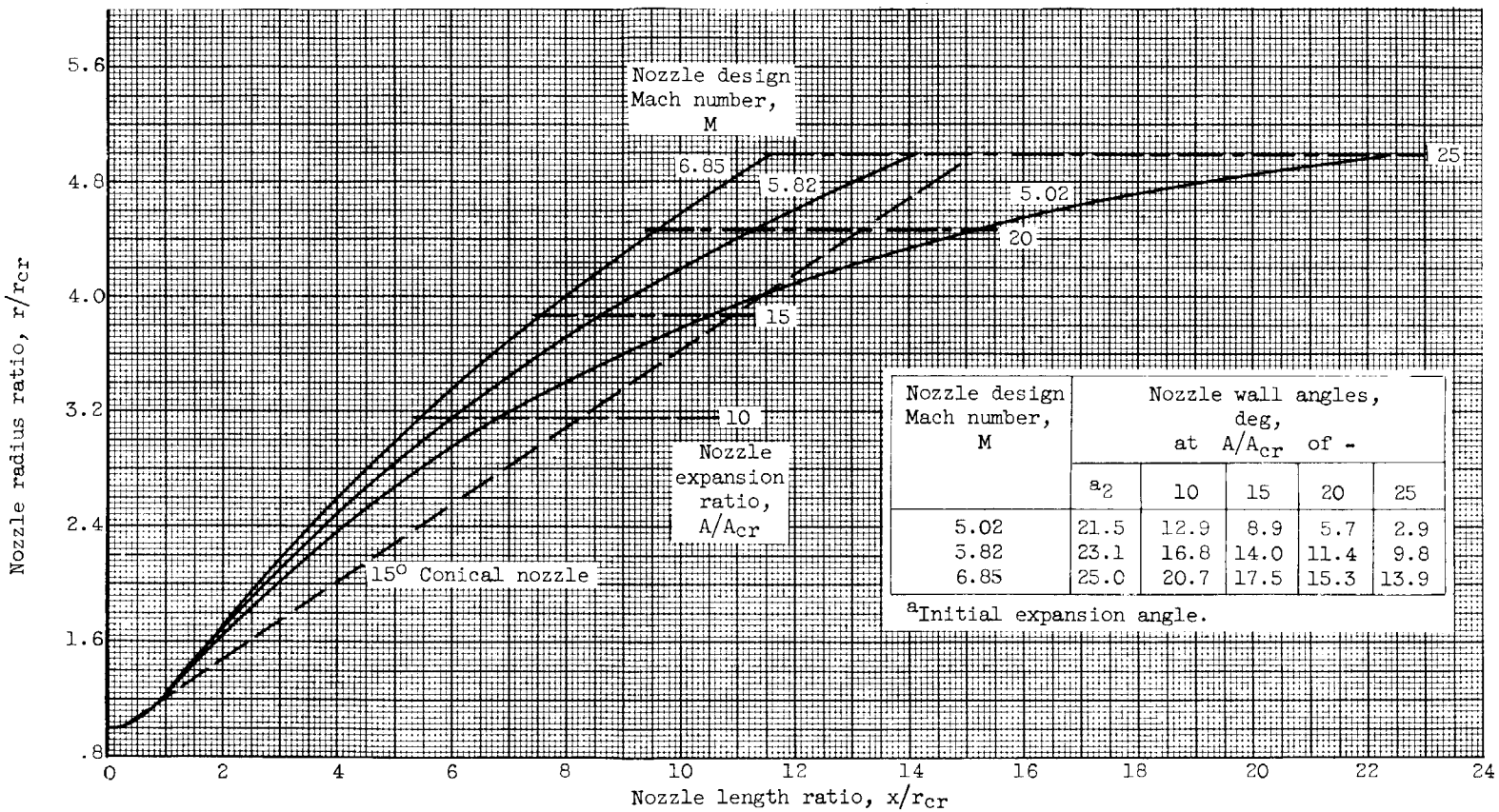

Nozzle design Mach number, M	Nozzle wall angles, deg, at A/A_{cr} of -				
	a_2	10	15	20	25
5.02	21.5	12.9	8.9	5.7	2.9
5.82	23.1	16.8	14.0	11.4	9.8
6.85	25.0	20.7	17.5	15.3	13.9

[a]Initial expansion angle.

Figure 2. - Isentropic nozzle contours including boundary-layer displacement-thickness correction.

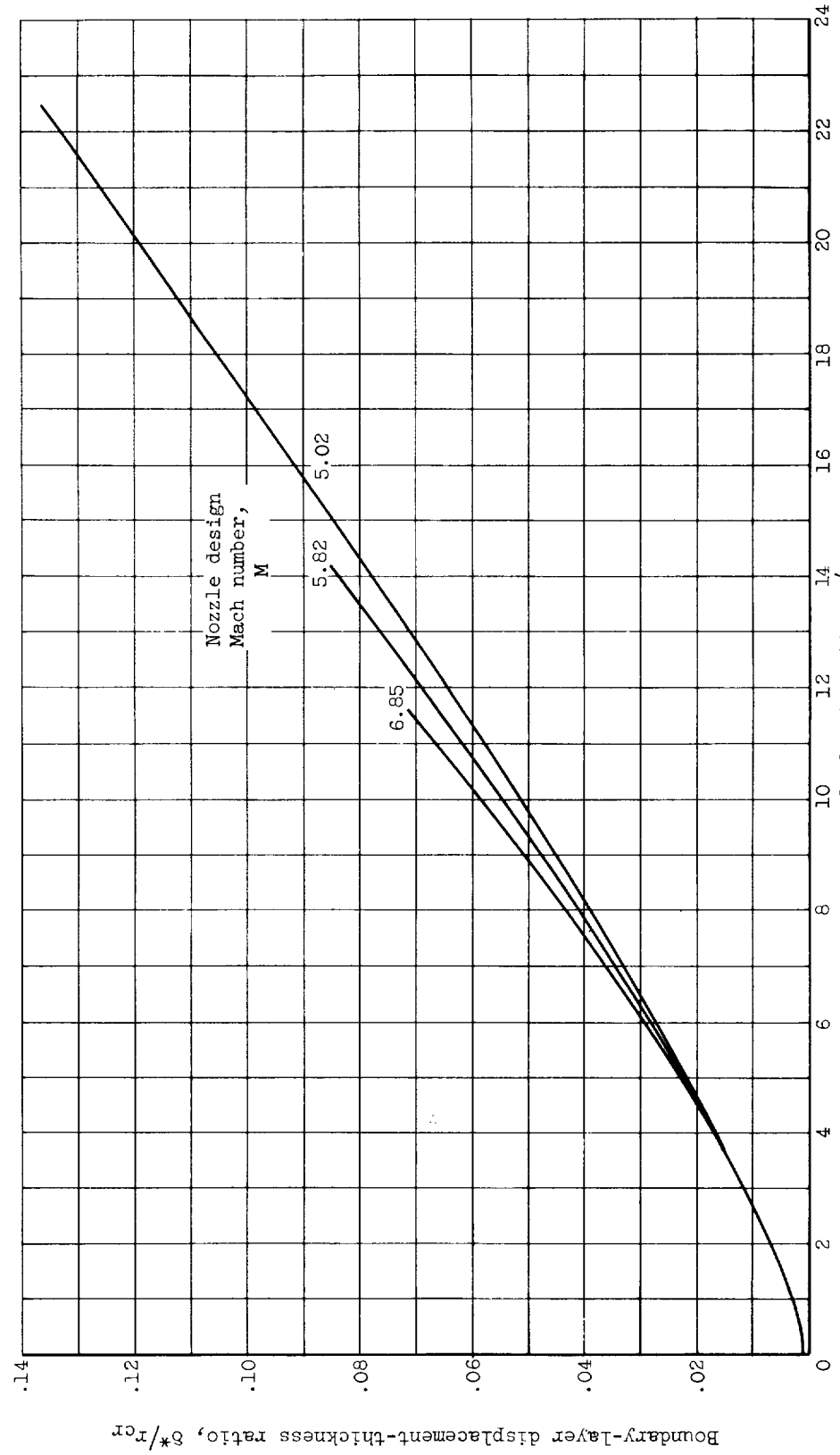

Figure 3. - Variation of boundary-layer displacement thickness with nozzle length.

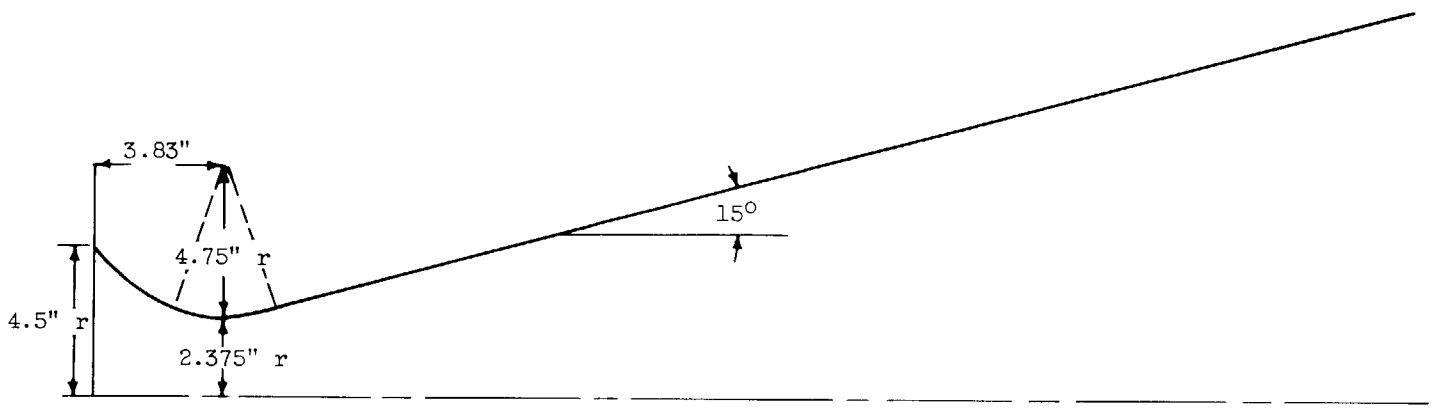

Nozzle expansion ratio, A/A_{cr}	Number of wall static taps	Nozzle expansion ratio, A/A_{cr}	Number of wall static taps
1.000	4	10.525	1
1.042	1	11.530	1
1.201	1	12.515	1
1.450	1	13.530	1
2.004	1	14.530	1
2.481	1	15.500	1
3.002	1	16.340	1
3.489	1	17.520	1
3.999	1	18.530	1
4.540	1	19.520	1
5.043	1	20.540	1
5.516	1	21.530	1
6.524	1	22.530	1
7.523	1	23.530	1
8.502	1	24.530	4
9.506	4		

Figure 4. - 15°-Conical-nozzle dimensions and instrumentation. (Location of nozzle wall static taps applies to all nozzles.)

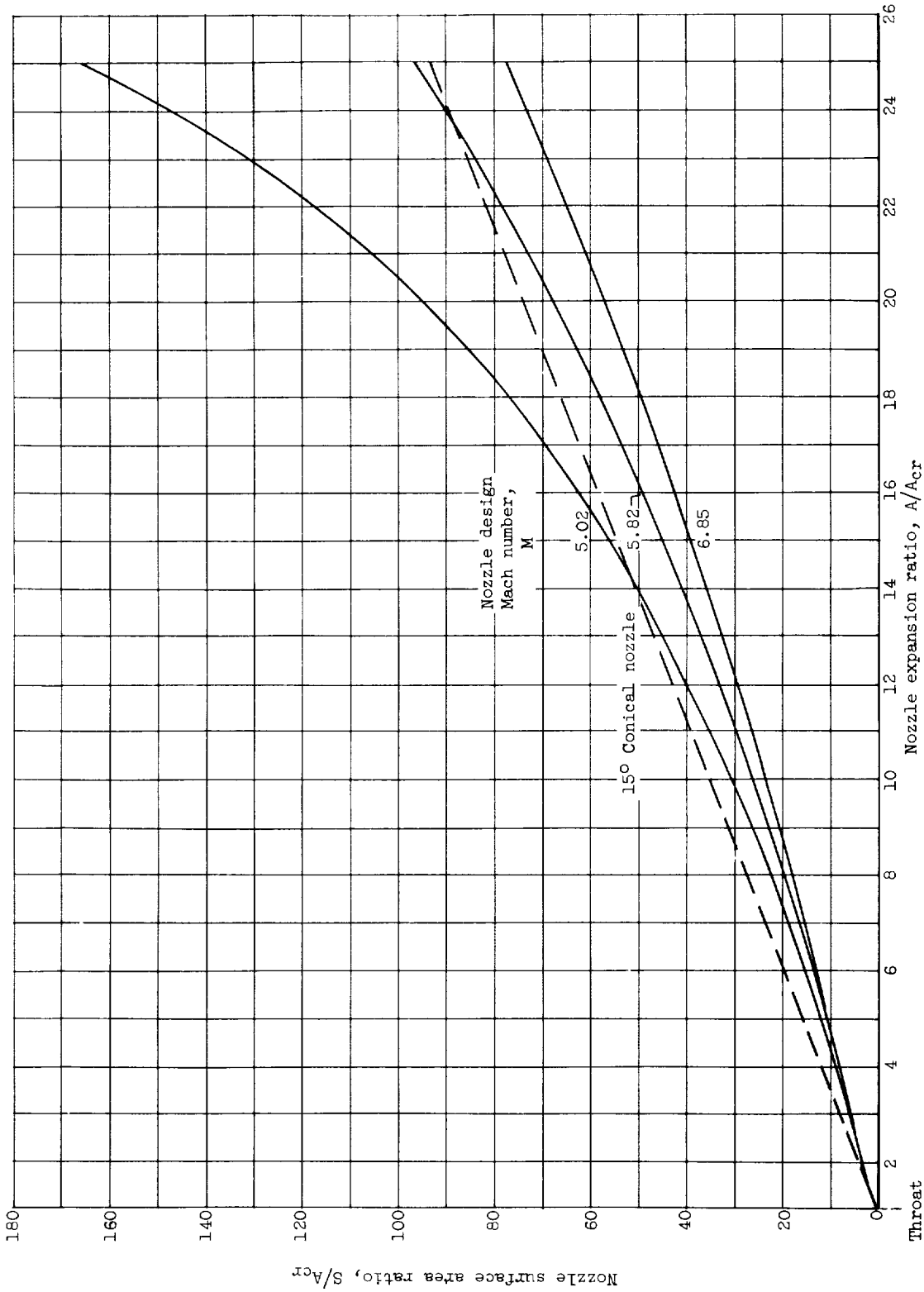

Figure 5. - Variation of nozzle surface area ratio with expansion ratio.

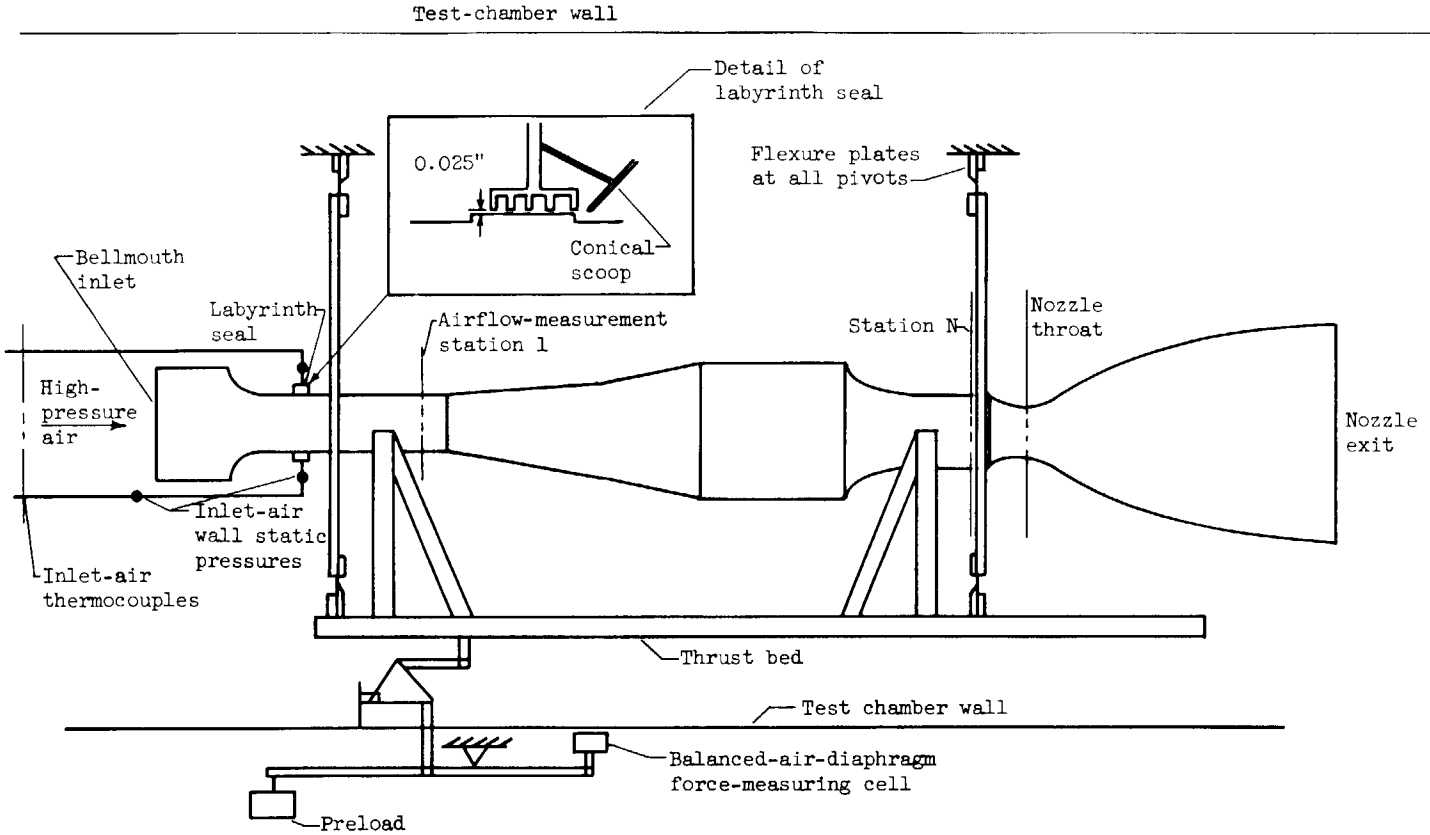

Station	Number of probes		Number of boundary-layer rakes
	Total pressure	Wall static pressure	
Airflow, 1	12	6	3
Nozzle inlet, N	20	6	1
Tank ambient, a	--	4	---

Figure 6. - Schematic diagram of nozzle test installation showing instrumentation location.

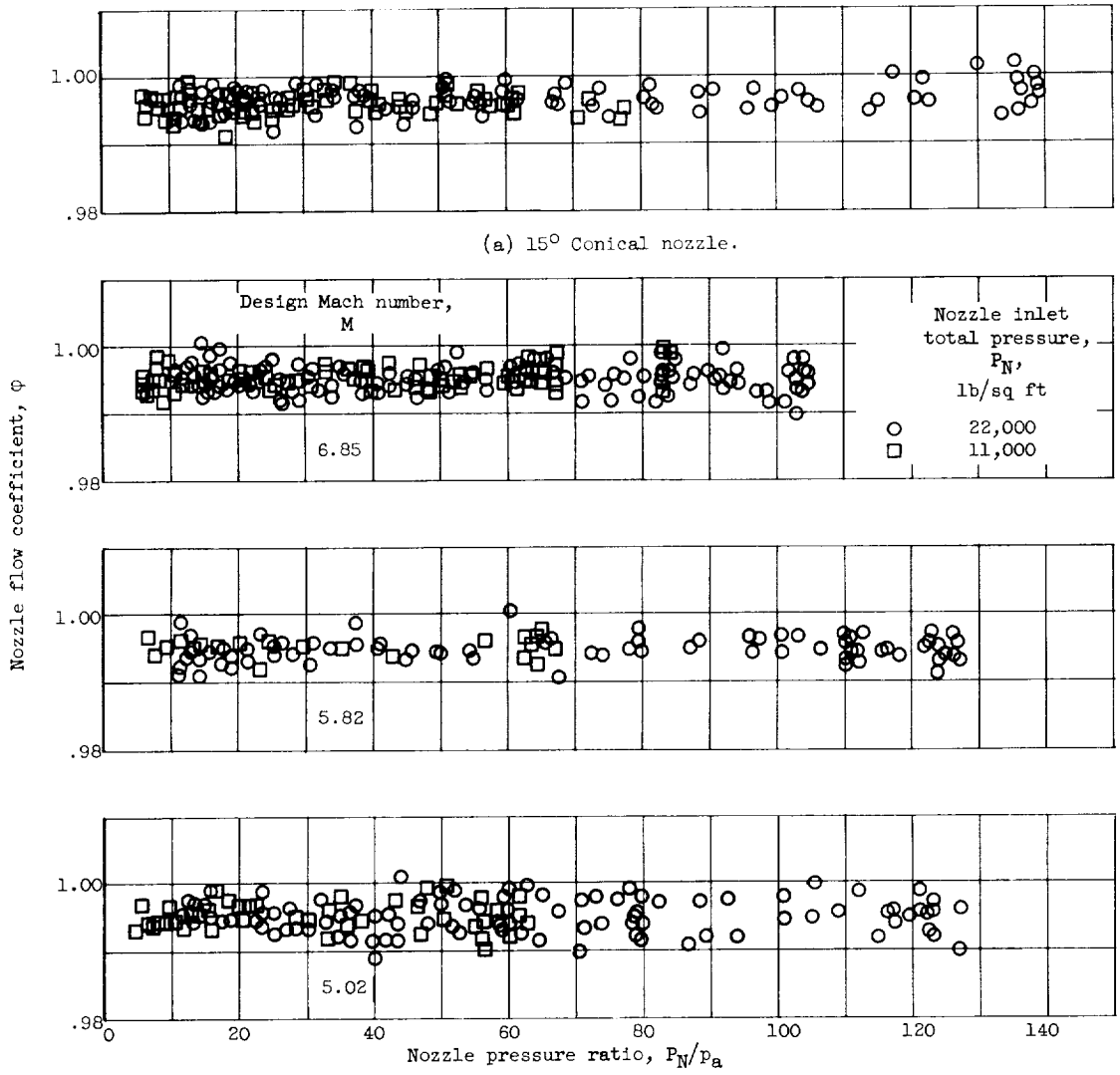

(b) Method-of-characteristics nozzles.

Figure 7. - Nozzle flow coefficients.

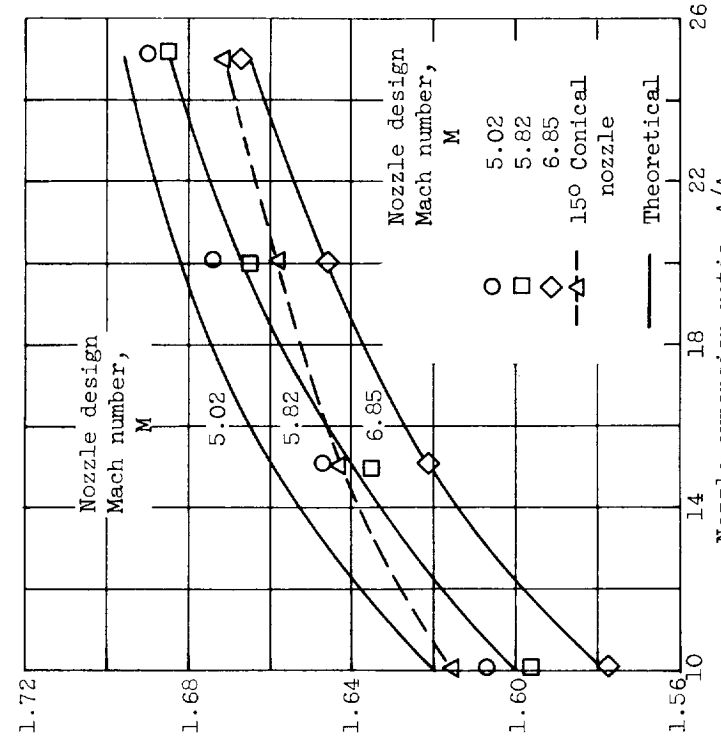

Figure 9. - Comparison of measured nozzle momentum with momentum calculated from theoretical nozzle static-pressure distributions.

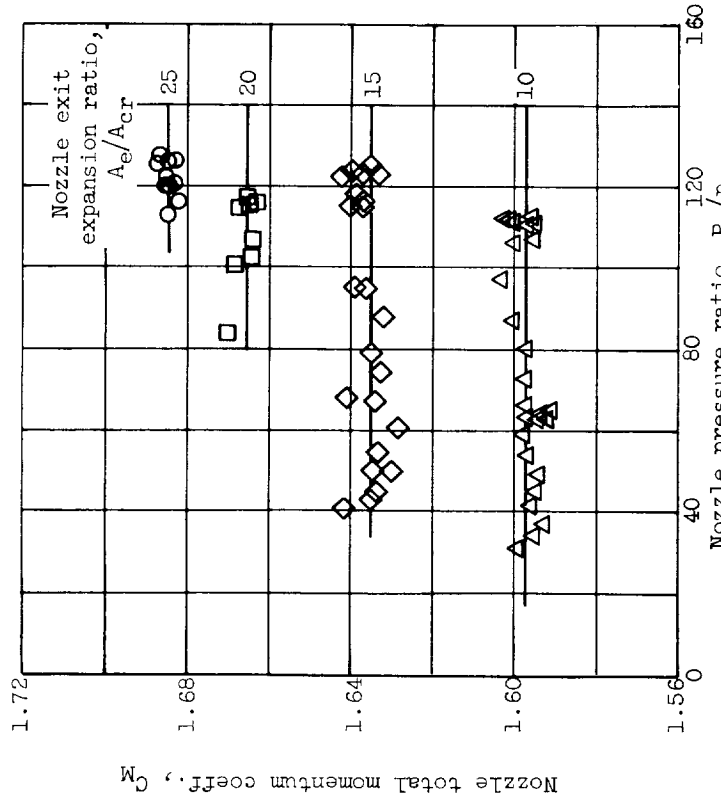

Figure 8. - Nozzle total momentum ratio computed from measured thrust. Nozzle design Mach number, 5.82.

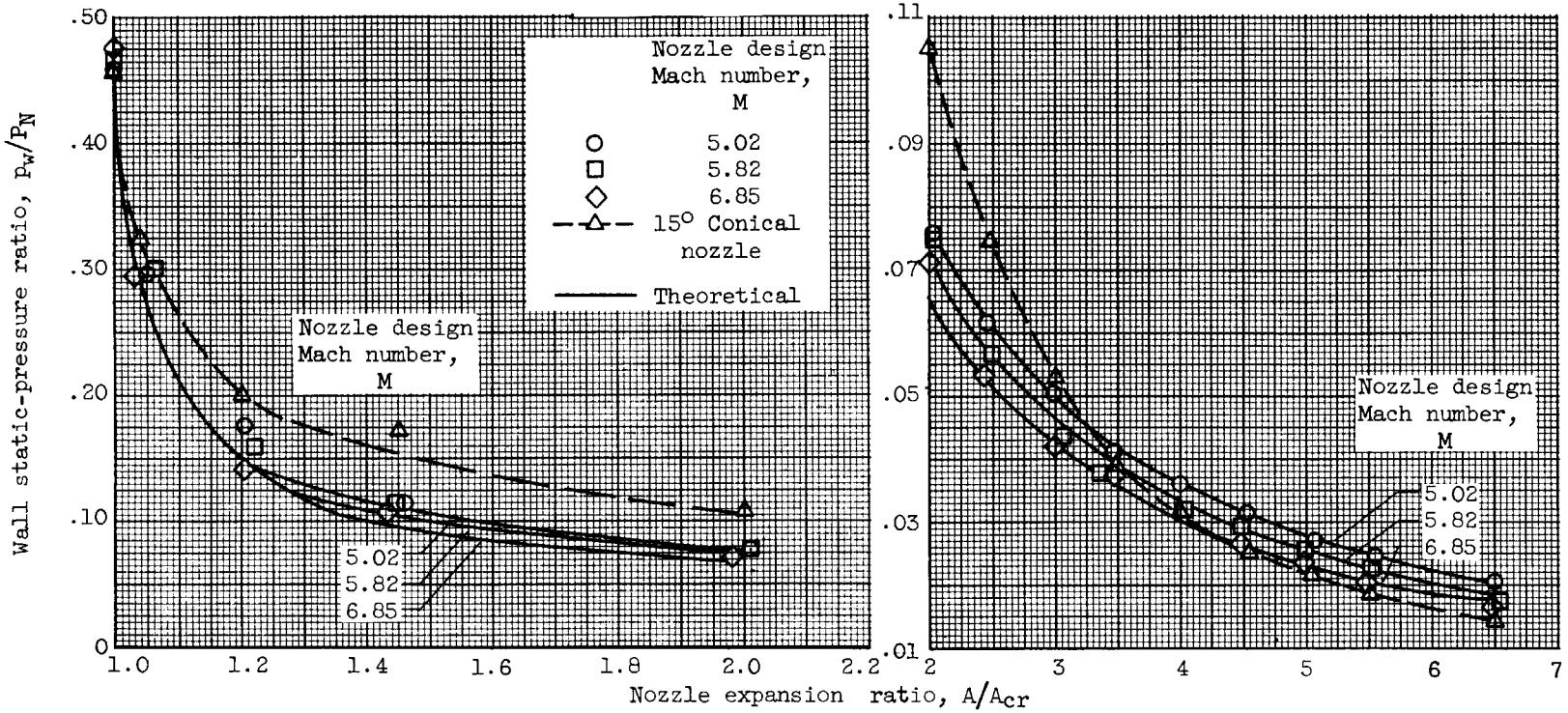

(a) Nozzle expansion ratio, 1.0 to 2.0.

(b) Nozzle expansion ratio, 2.0 to 6.5.

Figure 10. - Nozzle wall static-pressure distribution.

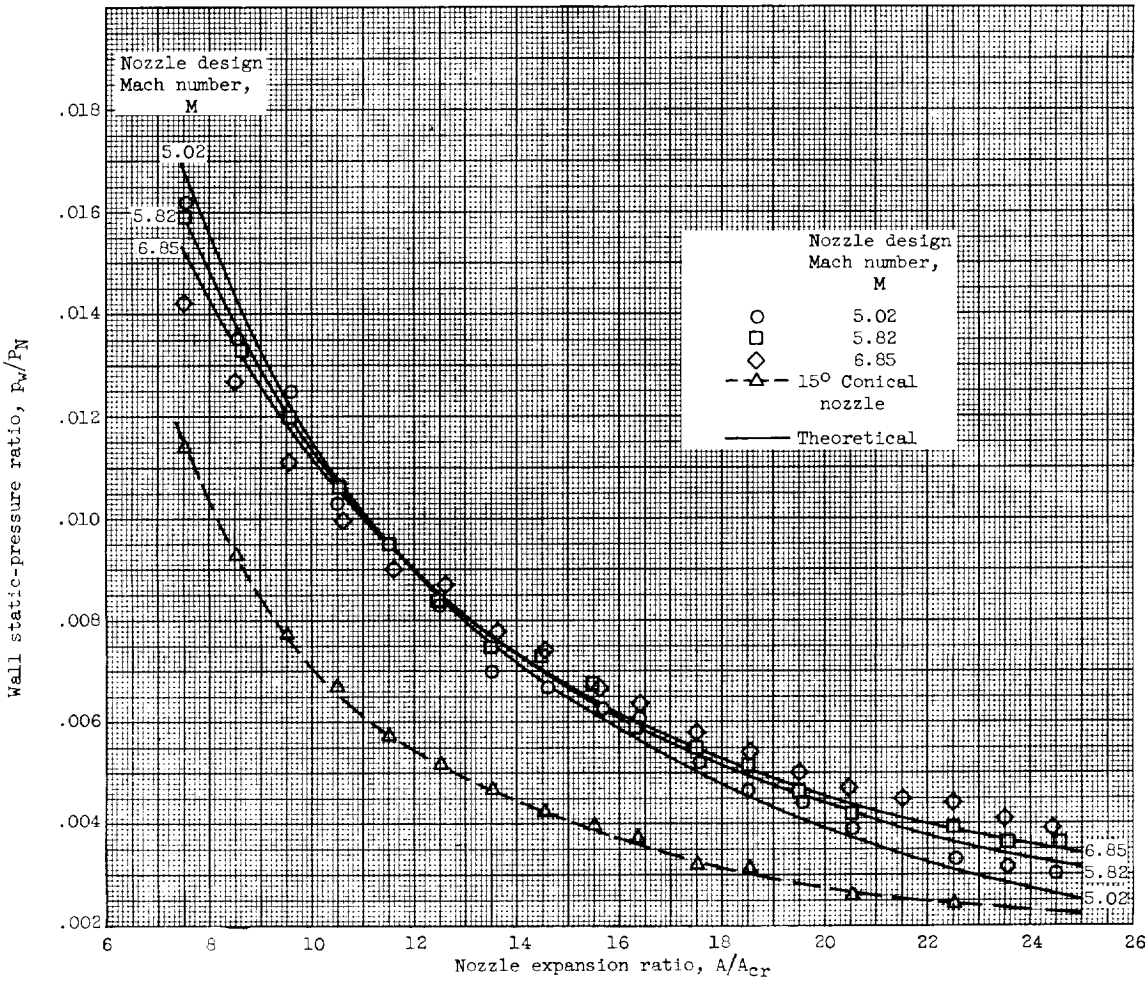

(c) Nozzle expansion ratio, 7.5 to 25.

Figure 10. - Concluded. Nozzle wall static-pressure distribution.

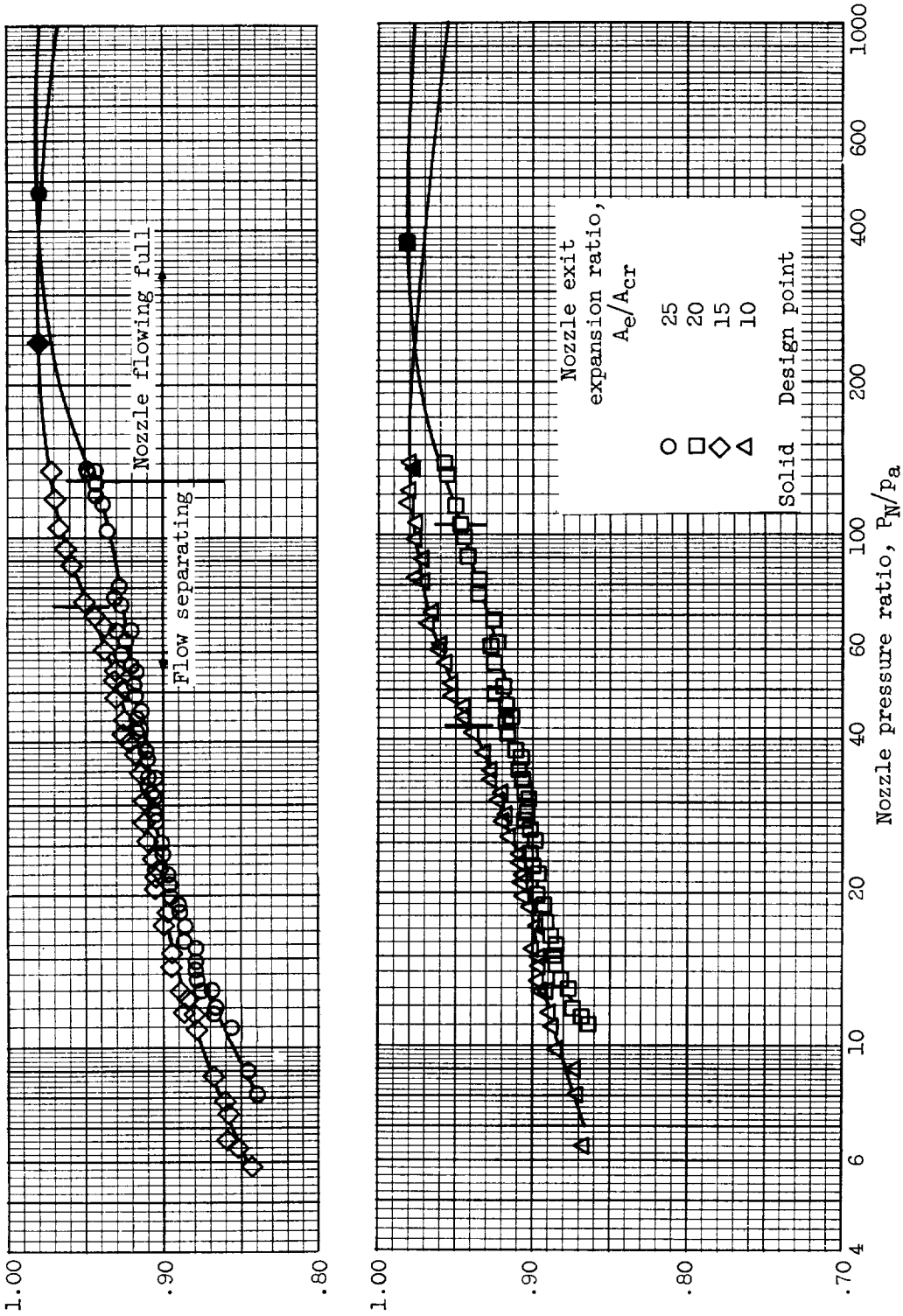

(a) 15° Conical nozzle.

Figure 11. - Variation of nozzle thrust ratio with nozzle pressure ratio.

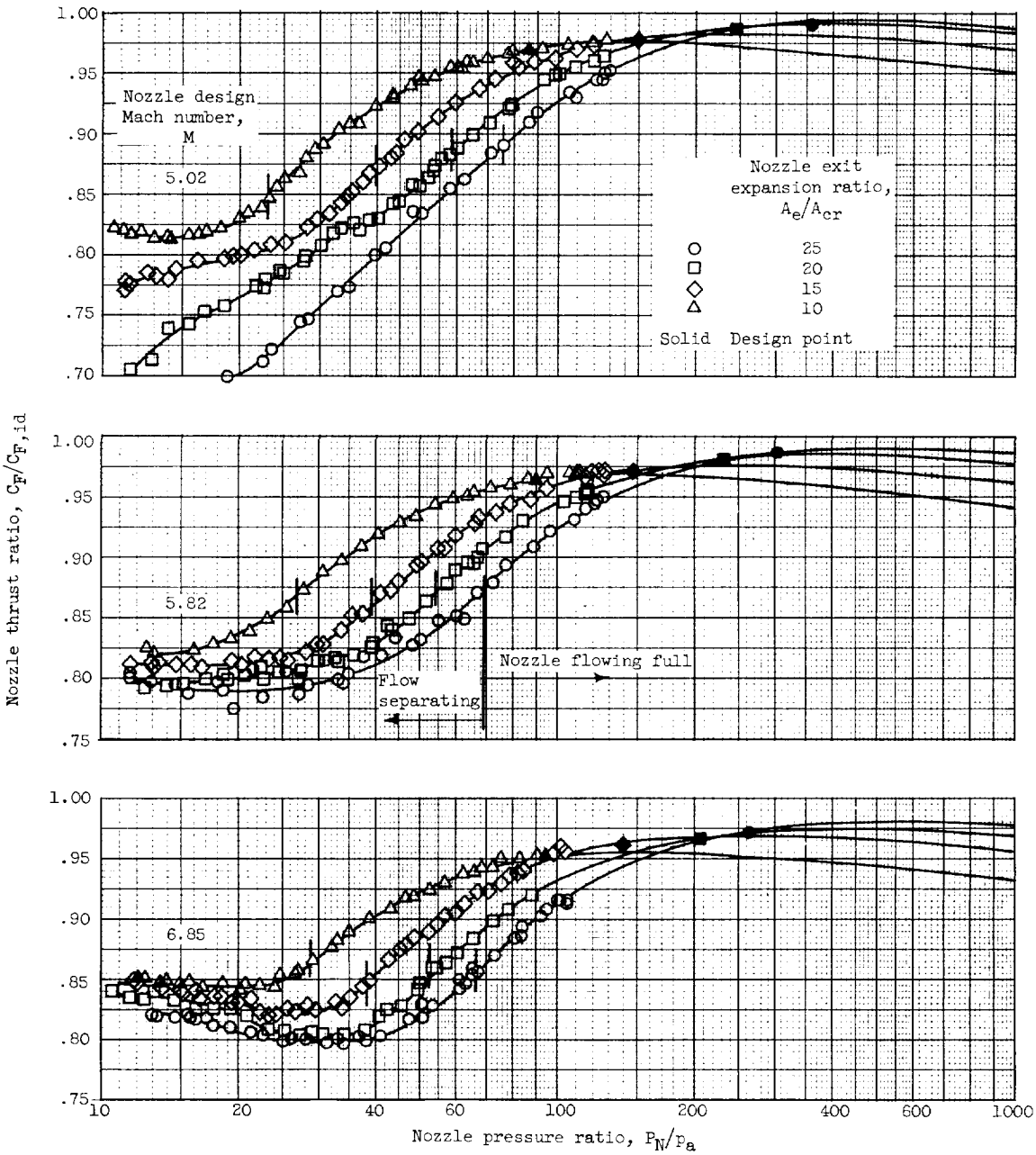

(b) Method-of-characteristics nozzles.

Figure 11. - Concluded. Variation of nozzle thrust ratio with nozzle pressure ratio.

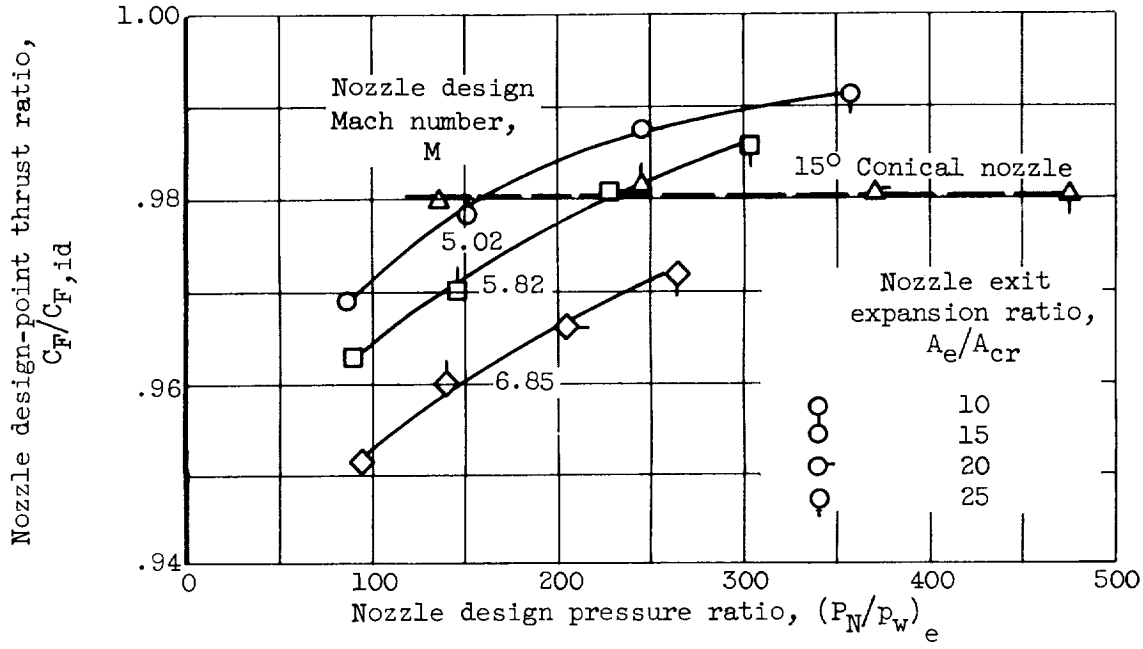

Figure 12. - Variation of design-point thrust ratio with design pressure ratio.

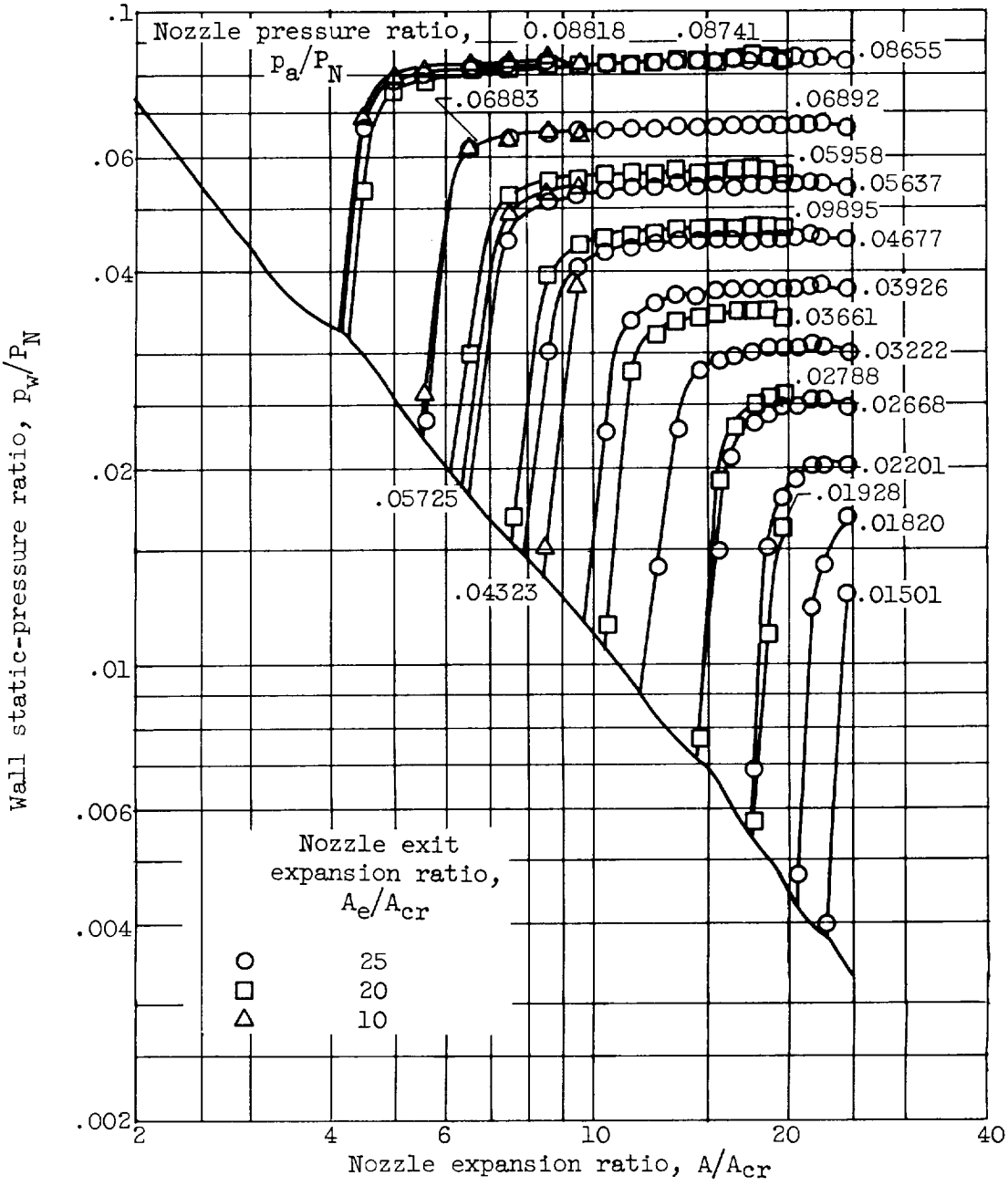

(a) Nozzle design Mach number, 5.82.

Figure 13. - Nozzle wall static-pressure distributions.

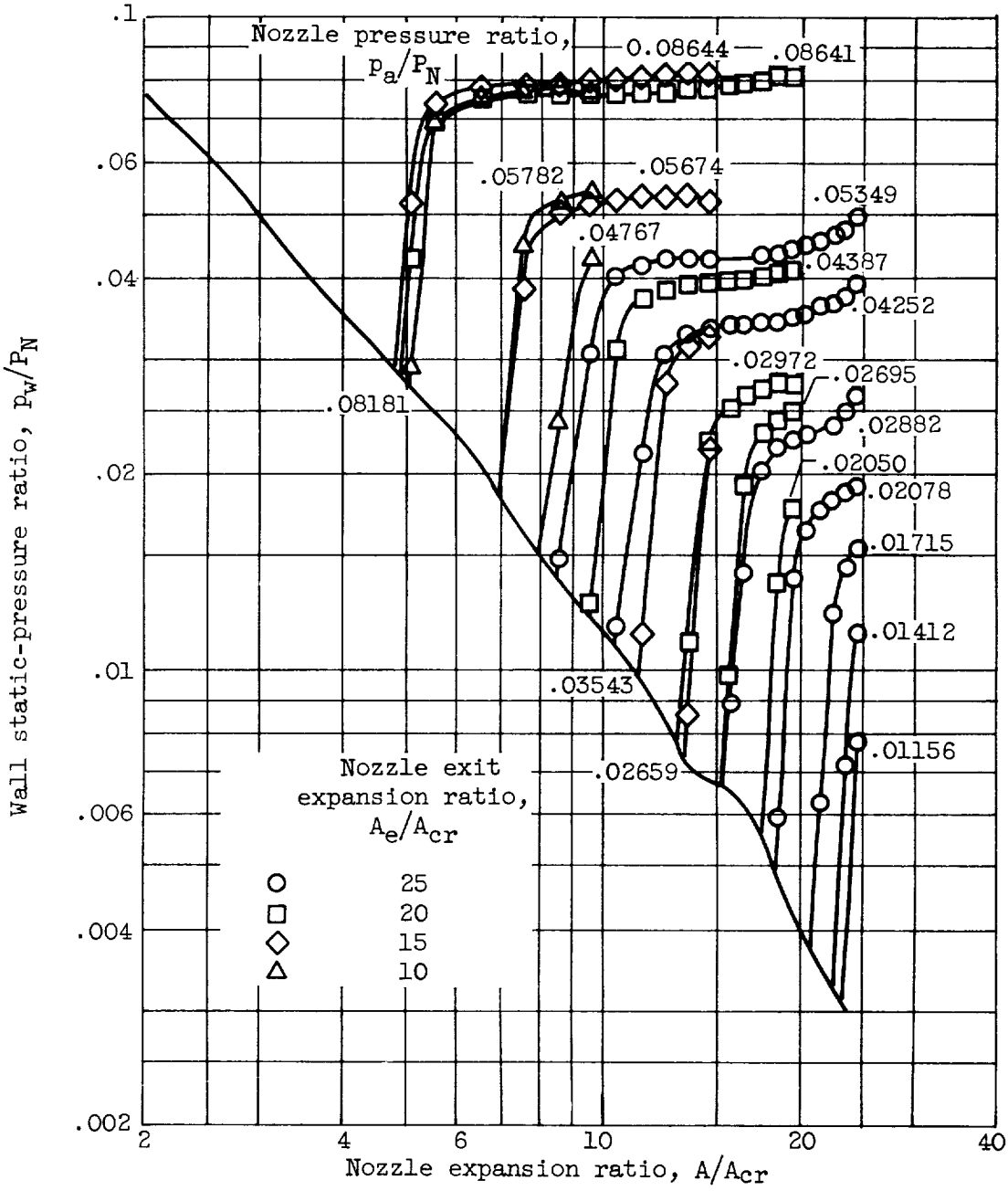

(b) Nozzle design Mach number, 5.02.

Figure 13. - Concluded. Nozzle wall static-pressure distributions.

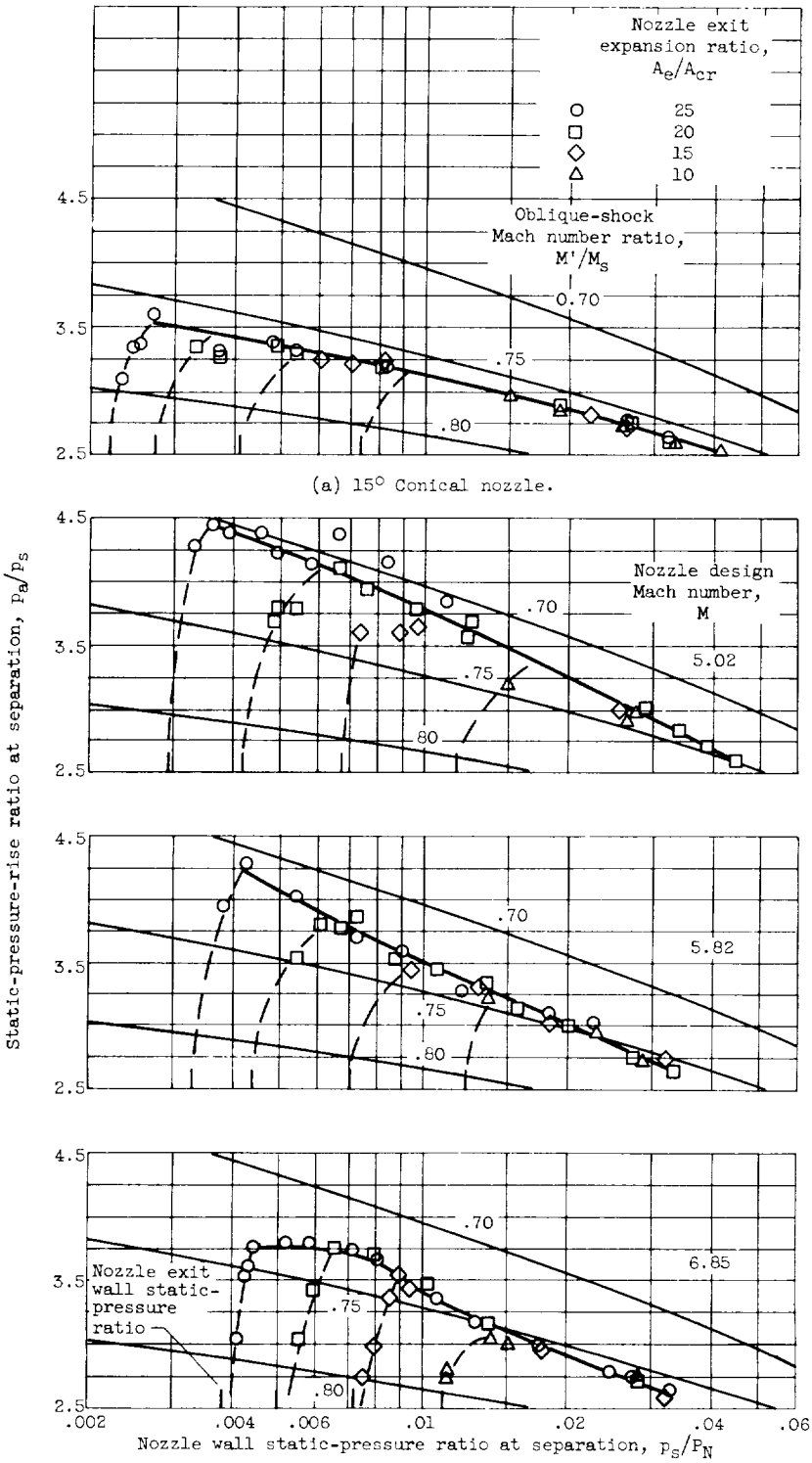

(a) 15° Conical nozzle.

(b) Method-of-characteristics nozzles.

Figure 14. - Variation of pressure-rise ratio at separation with nozzle wall static-pressure ratio at separation.

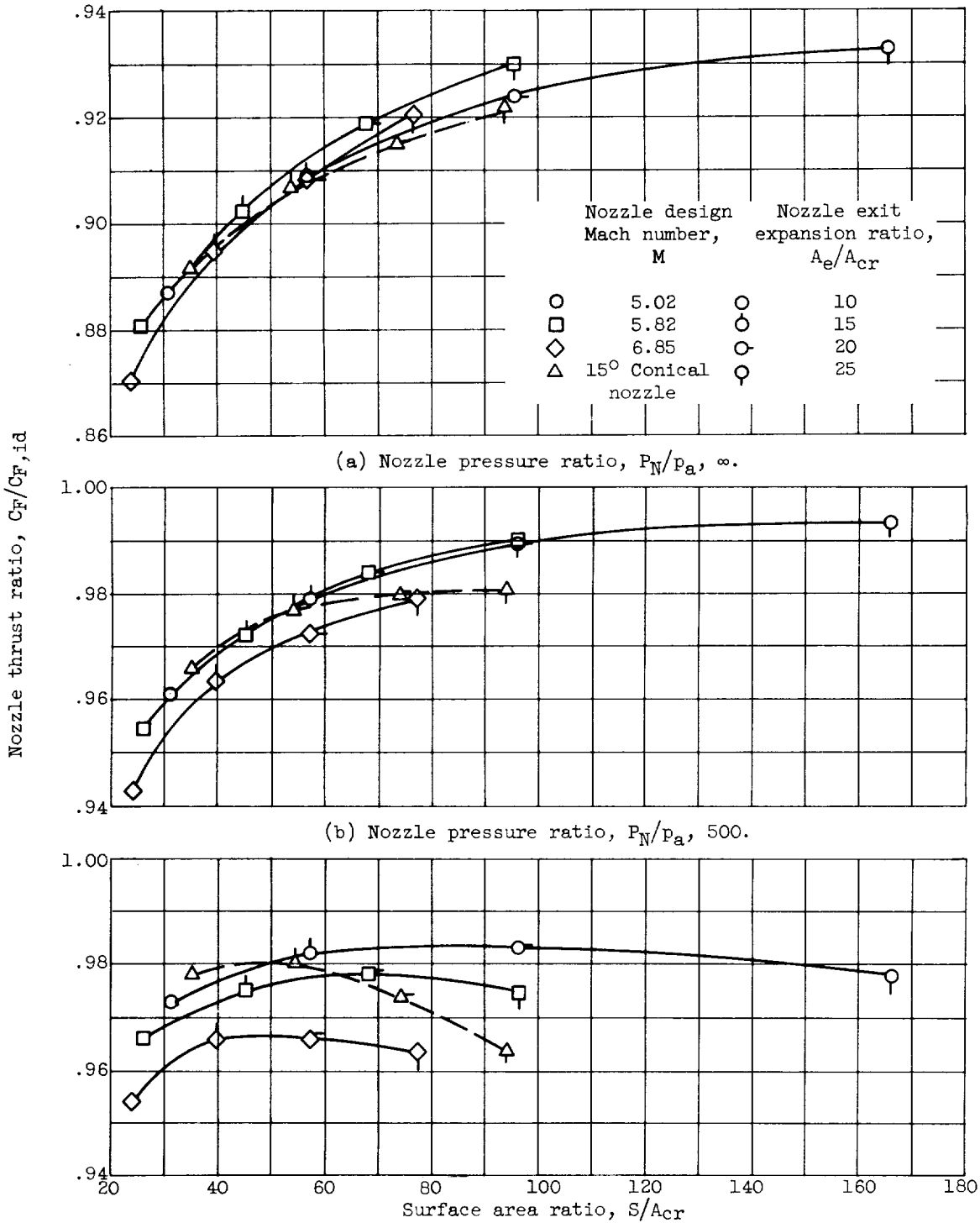

(a) Nozzle pressure ratio, P_N/p_a, ∞.

(b) Nozzle pressure ratio, P_N/p_a, 500.

(c) Nozzle pressure ratio, P_N/p_a, 200.

Figure 15. - Variation of nozzle thrust ratio with nozzle surface area ratio.

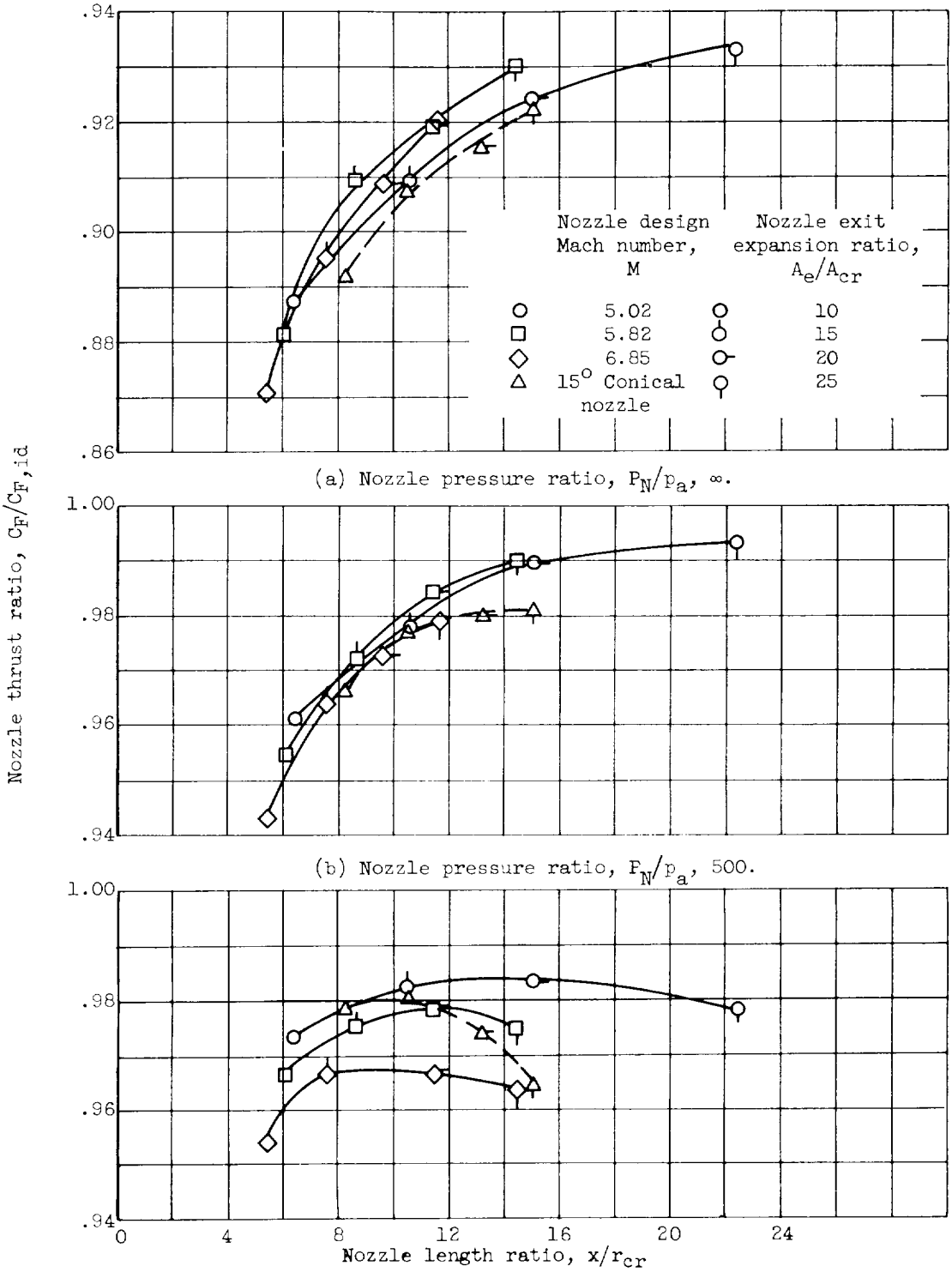

Figure 16. - Variation of nozzle thrust ratio with nozzle length ratio.

NASA TN D-293
National Aeronautics and Space Administration.
PERFORMANCE OF SEVERAL METHOD-OF-CHARACTERISTICS EXHAUST NOZZLES. John M. Farley and Carl E. Campbell. October 1960. 33p. OTS price, $1.00. (NASA TECHNICAL NOTE D-293)

Nozzle performance data were obtained with three "method-of-characteristics" nozzles and a 15° conical nozzle at pressure ratios up to 130. Each basic configuration was cut off and tested at expansion ratios of 25, 20, 15, and 10. As much as 1 percent increase in thrust, with no increase in nozzle surface area (weight), can be obtained by using a method-of-characteristics nozzle instead of a 15° conical nozzle when operating with a nozzle expansion ratio of 25. Theoretical and measured nozzle momentum coefficients agreed within about 0.6 percent.

Copies obtainable from NASA, Washington

I. Farley, John M.
II. Campbell, Carl E.
III. NASA TN D-293

(Initial NASA distribution: 37, Propulsion system elements.)

NASA

NASA TN D-293
National Aeronautics and Space Administration.
PERFORMANCE OF SEVERAL METHOD-OF-CHARACTERISTICS EXHAUST NOZZLES. John M. Farley and Carl E. Campbell. October 1960. 33p. OTS price, $1.00. (NASA TECHNICAL NOTE D-293)

Nozzle performance data were obtained with three "method-of-characteristics" nozzles and a 15° conical nozzle at pressure ratios up to 130. Each basic configuration was cut off and tested at expansion ratios of 25, 20, 15, and 10. As much as 1 percent increase in thrust, with no increase in nozzle surface area (weight), can be obtained by using a method-of-characteristics nozzle instead of a 15° conical nozzle when operating with a nozzle expansion ratio of 25. Theoretical and measured nozzle momentum coefficients agreed within about 0.6 percent.

Copies obtainable from NASA, Washington

I. Farley, John M.
II. Campbell, Carl E.
III. NASA TN D-293

(Initial NASA distribution: 37, Propulsion system elements.)

NASA

NASA TN D-293
National Aeronautics and Space Administration.
PERFORMANCE OF SEVERAL METHOD-OF-CHARACTERISTICS EXHAUST NOZZLES. John M. Farley and Carl E. Campbell. October 1960. 33p. OTS price, $1.00. (NASA TECHNICAL NOTE D-293)

Nozzle performance data were obtained with three "method-of-characteristics" nozzles and a 15° conical nozzle at pressure ratios up to 130. Each basic configuration was cut off and tested at expansion ratios of 25, 20, 15, and 10. As much as 1 percent increase in thrust, with no increase in nozzle surface area (weight), can be obtained by using a method-of-characteristics nozzle instead of a 15° conical nozzle when operating with a nozzle expansion ratio of 25. Theoretical and measured nozzle momentum coefficients agreed within about 0.6 percent.

Copies obtainable from NASA, Washington

I. Farley, John M.
II. Campbell, Carl E.
III. NASA TN D-293

(Initial NASA distribution: 37, Propulsion system elements.)

NASA

NASA TN D-293
National Aeronautics and Space Administration.
PERFORMANCE OF SEVERAL METHOD-OF-CHARACTERISTICS EXHAUST NOZZLES. John M. Farley and Carl E. Campbell. October 1960. 33p. OTS price, $1.00. (NASA TECHNICAL NOTE D-293)

Nozzle performance data were obtained with three "method-of-characteristics" nozzles and a 15° conical nozzle at pressure ratios up to 130. Each basic configuration was cut off and tested at expansion ratios of 25, 20, 15, and 10. As much as 1 percent increase in thrust, with no increase in nozzle surface area (weight), can be obtained by using a method-of-characteristics nozzle instead of a 15° conical nozzle when operating with a nozzle expansion ratio of 25. Theoretical and measured nozzle momentum coefficients agreed within about 0.6 percent.

Copies obtainable from NASA, Washington

I. Farley, John M.
II. Campbell, Carl E.
III. NASA TN D-293

(Initial NASA distribution: 37, Propulsion system elements.)

NASA